3

Assessment of Stereoscopic Precision – Film to Digital Photogrammetric Cameras

Benjamín Arias-Pérez[1], Diego González-Aguilera[1], Javier Gómez-Lahoz[1] and David Hernández-López[2]
[1]High Polytechnic School of Avila, Department of Cartographic and Land Engineering, University of Salamanca
[2]Regional Development Institute, Albacete, University of Castilla-La Mancha
Spain

1. Introduction

In the generation of the three more important photogrammetric products, digital terrain models (DTM), orthophotos and maps derived from compilation, issues such as direct georeferencing, managing a high volume of data and automatic measurements (matching), are really important. However, within the photogrammetric workflow still exists tasks that remain manual or that require user interaction. The generation of cartography through restitution is one of the tasks that require an intense user interaction despite the great advances in the sector. On the other hand, the constant emergence of new large and medium format digital sensors and their incorporation into large photogrammetric projects has prompted different stakeholders demand and thus a greater need to the knowledge of the precision, correctness and reliability of these sensors, especially when most existing photogrammetric software do not allow a detailed analysis of the results. That is why nowadays is still relevant to consider the photogrammetric precision reached by an operator measuring on a digital image and compare it with that achieved by measuring on a scanned film image, considering always that both dataset are provided with similar input conditions (pixel size, measurement device, expertise of the operator, etc.)

This chapter aims to address this issue in detail through a study of manual stereoscopic precision measured on original digital image and digitalized film images. After this introduction, Section 2 will address a comprehensive bibliographic review of major studies in this line, from those made in the field of analogical photogrammetry to the modern large-format digital cameras. Section 3 will describe in detail the main materials and methods used in this study. Section 4 will focus on showing experimental results obtained in three different study cases with a discussion of them. The last section we will highlight the main concluding remarks from this study.

2. State of the art

Photogrammetric Community has always tested new tools and methods with the aim of guaranteeing that the results achieved are equal to or better than traditional ones. In this sense, one of the first tests performed was to check the precision of the film cameras that finally replaced the plate cameras (Grifoni, 1949). From these studies important conclusions were derived confirming the superiority of the plate cameras in terms of precision. However, for small and medium scales, film cameras were fully reliable. Later, Lehmann (1955) in the framework of the Organisation Europeenne d'Etudes Photgrammetriques Experimental OEEPE investigates the precision of restitution based on several factors such as the field of view, photographic material (film or plate), the method of measuring, the user, the type of instrument (plotter, etc.). To develop this work, Switzerland offered a test field located in the Rhine valley near Oberriet, which covers an area of 1,5 x1,5 km with 600 control marks with planimetric and altimetric coordinates. Furthermore, in an area of 4x4 km points were spaced every 500 m. This trend was followed by a total of 7 schools in different countries (1 in Switzerland, Austria, Italy and the Netherlands and three in Germany), using different restitution instruments. Some of the centers that performed the measurements published their reports including aspects such as: times of measurement, methods of operation, problems encountered and their solutions, and even the measurements made by the operators (Gotthardt, 1955; Brucklacher, 1955, and Förstner, 1955, Commission C., Ablauf der Messung OEEPE Deroulment Zeitlicher chronologique des observations, 1955), while the results were discussed in later publications (Gotthardt, 1958, and Stickler, 1959; Stoch, 1961). At the same time as the OEEPE began its work, the International Society of Photogrammetry, ISP, showed their concerns about the restitution of cadastral maps (Härry, 1954), land consolidation (Härry, 1955), establishing plans for urban areas (Dubuisson, 1955) and small scale mapping (Blachut, 1955). In 1975, the analysis of planimetric and altimetric precision on the restitution was revived again but this time through the angular field factor. Stark (1975) used a total of 4 cameras with varying focal lengths and taking images at different flight altitudes. A total of 23 sets of points distributed regularly around the stereoscopic model were measured and analyzed for each stereoscopic model. The study followed that the altimetric mean error decreases continuously as the image angle increases, while the planimetric mean error is practically independent of this angle. On the other hand, another aspect that has provided a particular interest from the International Photogrammetric Community is the comparison of stereoscopic and monoscopic measurements (O´Connor, 1967; Karara, 1967; Trinder, 1986). To this end, manual stereoscopic measurements involving human operators were also developed in some tests to determine the stereoscopic accuracy achieved by restitution operators (Zorn, 1965, Krakau, 1970).

With the advent of large format digital cameras in 2000, studies comparing the analog-digital technology have become inevitable. Dörstel (2003) analyzed the precision of large-format digital camera DMC using four flights at different heights while preserving the ratio of base/height (*b/h*). Dörstel performed 10 measurements of each point and use different types of points that allow him to contrast the empirical and theoretical precision. Alamús et al. (2005) contrasted the ground coordinates (measured with GPS) with those obtained by stereoscopic measurement, and making these measurements with film camera, RC30 (b/h=0,6), and digital, DMC (b/h=0,3). Use 11 points in a flight with a GSD of 0,08 m (Amposta block), and 21 points on another flight of 0,5 m (Caro block). It provides data on how many times are measured points, or if they are homogeneously distributed in the model, or classified in some way, how many operators are involved in the measurements, etc. The results show that the smallest ratio *b/h* for DMC camera is compensated with higher precision in stereo measurements, reaching comparable values in all components (*X,Y,H*), and for the two flights. Subsequently, other specific tests were performed to determine the altimetric stereoscopic precision. Points were measured in several contiguous stereo models near to the so-called Von Gruber points. The results showed that the precision in *Z* is worse in the case of digital camera which can be due to the topography, or because that overlap areas are different in digital and film images.

More recently, Arias and Gomez-Lahoz (2009) conducted an empirical study of stereoscopic precision. Finally, Spreckels et al. (2010) reported the results obtained in the project DGPF "Evaluation of Digital Photogrammetric Camera Systems", within the working group "stereoplotting". Multiple cameras were used in this project: Film Camera Zeiss RMK Top 15; large format digital cameras UltraCamX Vexcel Imaging and Intergraph / ZI DMC, and the combination of four medium format cameras Digi-CAM Quattro IGI. The main outline of the project show a precision better than 0,9 pixel in *XY* and 1,4 pixel in *Z*.

3. Materials and methods

3.1 Photogrammetric sensors: Digital

3.1.1 DMC

This digital sensor is based on a multi-cone matrix, so that four sensors can provide a large format CCD (7.000 x 4.000-pixel, 12 micron pixel size), which capture the image at the same time (synchronous operation) (Fig. 1). Panchromatic cones are slightly inclined, so they have a small common area, which is then used to generate the so-called virtual image size of 13.824 x 7.680 pixels (height x width). The color information is obtained from four CCDs with a smaller size, but that capture the entire scene. A whole high-resolution color image can be obtained automatically using pan-sharpening method.

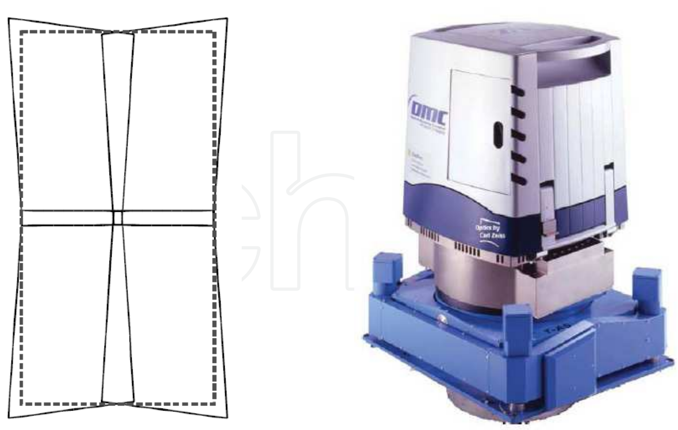

Fig. 1. Left: images of the four cones (solid line), and the virtual image (dashed line).
Right: DMC digital camera.

3.1.2 UltraCam

The UltraCamD camera design is based on the use of 9 sensors CCDs (each of 4.000 x 2.700 pixels) with pixel size of 9 microns (Fig. 2). Each cone has the same field, but the CCDs are arranged in various positions within the focal plane. The idea is that not all cones are exposed to the same time, but at the same place (operation syntopic). A cone acts as a master cone, and that defines the image coordinate system. The other images are paired as secondary parts in this main frame defined by the master cone. The final image has a single central perspective and has a size of 11.500 x 7.500 pixels.

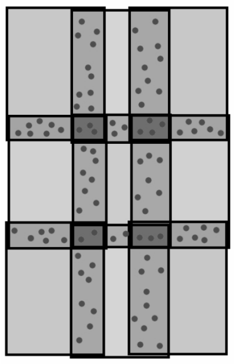

Fig. 2. Left: 9 CCDs that form the complete image of the camera UltraCam.
Right: camera UltraCamD.

3.2 Photogrammetric sensors: Film

In this case the camera used was the Leica RC30 camera, widely used in aerial photogrammetry industry. It allows two settings: 15/4 UAG-S with a focal length of 15 cm (the one used in the measurements), and 30/4 NAT-S with a focal length of 30 cm. In both cases, the format corresponds to a film width of 240 mm. But due to the intrinsic characteristics of these cameras (fiducial marks, marginal information) the effective width is smaller.

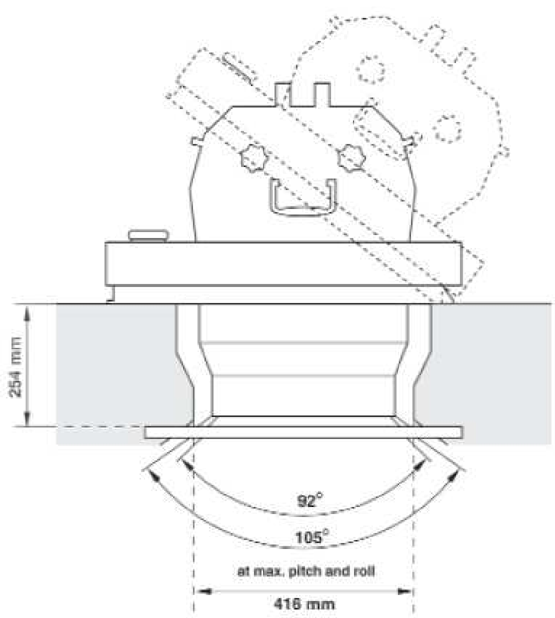

Fig. 3. Left: diagram of Leica RC30 with 15/4 UGS (in PAV30 mount). Right: Leica RC 30 camera (in PAV30 mount) and the NSF3-E Navigation Sight.

The scanner used to convert the film to digital format was Vexcel UltraScan 5000.

3.3 Methods

The following precision analysis have been established in this study: *XY* precision, *Z* precision, relationship between planimetric and altimetric precision, comparison of means, analysis of agreement, personal equation and relative relief. Measurements were taken with the analytical plotter Leica SD2000 and the photogrammetric digital workstation Digi3D.

3.3.1 Theoretical precision in planimetry

The theoretical *XY* precision is directly proportional to the scale of the image, m_b, and the measurement precision of the image, σ_i:

$$\sigma_{xy} = \sigma_i * m_b \tag{1}$$

The precision of the measure on the image plane, σ_i usually ± 6µm (Kraus, 1993) can be expressed in terms of pixel size, *px*, as a fraction (*1/k*). This value *k* can be considered as an indicator of measurement precision in the image.

$$\sigma_i = \frac{px}{k} \Rightarrow \sigma_{xy} = \frac{px}{k} * m_b \tag{2}$$

Moreover, the product of pixel size for image scale provides the pixel size in the ground, *GSD (Ground Sample Distance)*:

$$GSD = px * m_b \Rightarrow \sigma_{xy} = \frac{GSD}{k} \tag{3}$$

Thus, the precision observed in *XY* can be expressed as a fraction of the *GSD*. Once the empirical planimetric standard deviation, S_{XY}, is obtained, the empirical measurement precision of the image, S_i is get. From S_i the value of *k* can be computed which is a good value of comparison between cameras.

$$\begin{gathered} S_{xy} = S_i * m_b \Rightarrow S_i = \frac{S_{xy}}{m_b} \\ S_i = \frac{px}{k} \Rightarrow k = \frac{px}{S_i} \end{gathered} \tag{4}$$

From this expression it follows that the higher *k*, the better precision.

It is important to note that σ expresses the theoretical precision while *S* expresses the empirical standard deviation which is determined from measurements.

3.3.2 Theoretical precision in altimetry

The theoretical precision in *Z*, σ_Z, depends on the precision of measurement of the horizontal parallax, σ_{Px}, the image scale, m_b, and the ratio height/base, *H/B* (Kraus, 1993; Schiewe, 1995):

$$\sigma_z = \sigma_{Px} * m_b * \frac{H}{B} \tag{5}$$

The measurement precision of the horizontal parallax can be replaced by the measurement precision in the image plane, σ_i. The ratio height/base can be replaced by the ratio focal/base (*c/b*), then:

$$\sigma_z = \sigma_i * m_b * \frac{c}{b} \tag{6}$$

The precision of the measure in the image plane, σ_i, can be expressed in terms of pixel size as a fraction of it. In this case, it is assigned a value of *1/k*:

$$\begin{aligned} \sigma_i &= \frac{px}{k} \\ \sigma_z &= \frac{px}{k} * m_b * \frac{c}{b} \end{aligned} \tag{7}$$

Moreover, the product of pixel size for image scale provides the pixel size in the ground, *GSD*:

$$\begin{aligned} GSD &= px * m_b \\ \sigma_z &= \frac{GSD}{k} * \frac{c}{b} \end{aligned} \tag{8}$$

As can be seen, precision in *Z* can also be expressed in terms of the *GSD*, the focal length and photobase. This is a function of longitudinal overlap, R_L, together with the image width:

$$b = (1 - R_L) * width \tag{9}$$

The value *c/b* affects proportionally the *Z* precision, so that the higher the value of this ratio less precision in *Z*.

Camera	*c (mm)*	*Width (mm)*	*b* (R_L *= 60%) (mm)*	*c/b*
Film	150	220	88	1,704
DMC	120	95	38	3,158
UltraCamD	100	67,5	27	3,704
UltraCamX	100	68,4	27,36	3,655

Table 1. Ratios *c/b* or various photogrammetric aerial cameras, calculated for a longitudinal overlap of 60%.

A comparison of details leads to the study of the ratio of precisions with two different cameras (*D*: Digital, UltraCamD or DMC; *A*: Analog-Film):

$$\frac{(\sigma_z)_D}{(\sigma_z)_A} \tag{10}$$

The comparison must be made by measurements from similar flights, which have the same *GSD*:

$$\frac{(\sigma_z)_D}{(\sigma_z)_A} = \frac{\left(\frac{GSD}{k} * \frac{c}{b}\right)_D}{\left(\frac{GSD}{k} * \frac{c}{b}\right)_A} = \frac{\left(\frac{1}{k} * \frac{c}{b}\right)_D}{\left(\frac{1}{k} * \frac{c}{b}\right)_A} \tag{11}$$

The ratios c/b are known for a camera, having determined their longitudinal overlap. At first, it is assumed that *k*, an indicator of precision is the same for both cameras. Then, it is determined the empirical *Z* precision of a digital camera (S_{ZD}), the empirical *Z* precision of a film camera (S_{ZA}) and their ratio:

$$\frac{(\sigma_z)_D}{(\sigma_z)_A} \neq \frac{(s_z)_D}{(s_z)_A} \Rightarrow k_D \neq k_A \tag{12}$$

Since *c/b* ratios are known for the two cameras, *k* which marks the measurement precision in the image plane is different for the two cameras (the higher *k*, the better precision). The following cases can be obtained:

- Theoretical ratio greater than the empirical one. As a result, the precision achieved in digital camera *Z* is greater than expected. Therefore, it is assumed that k_D is greater than k_A. This means that, somehow, the quality of the digital camera is better than can be expected theoretically.

$$\frac{(\sigma_z)_D}{(\sigma_z)_A} > \frac{(s_z)_D}{(s_z)_A} \Rightarrow k_D > k_A \tag{13}$$

- Theoretical ratio less than the empirical one. It is the opposite of the previous case, so the *Z* precision achieved in digital camera is smaller than expected. As a result the quality of the digital camera is worse than the film camera.

$$\frac{(\sigma_z)_D}{(\sigma_z)_A} < \frac{(s_z)_D}{(s_z)_A} \Rightarrow k_D < k_A \tag{14}$$

- There are no significant differences between the theoretical and the empirical ratio. There is no difference in the stereoscopic precision.

$$\frac{(\sigma_z)_D}{(\sigma_z)_A} \approx \frac{(s_z)_D}{(s_z)_A} \Rightarrow k_D \approx k_A \tag{15}$$

In the case of significant differences between the ratio of theoretical and empirical precision, a significant change in the quality of stereoscopic measurement is obtained, since the geometric basis of the ratio *c/b* is indisputable. Therefore, only *k* is an indicator of measurement precision in the image plane. If the measurements are made under the same conditions, the differences can be attributed not to the measurement in the image but the image quality itself. By and large, if significant or important differences are obtained between the empirical and theoretical ratio, a significant difference in image quality could be the reason.

3.3.3 Relationship between planimetric and altimetric precision

The ratio between the planimetric and altimetric precisions obtained, S_{XY}/S_Z, compared with the ratio *B/H*, expresses the variation between the planimetric and altimetric precisions. Since, theoretically, this ratio is unity:

$$\frac{S_{xy}/S_z}{\sigma_{xy}/\sigma_z} = \frac{S_{xy}/S_z}{(\sigma_i * m_b)/(\sigma_i * m_b * H / B)} = \frac{S_{xy}/S_z}{B/H} = 1 \tag{16}$$

Therefore, if the value for this ratio is less than one, this would indicate that planimetric precision is better than the altimetric precision. Otherwise (greater than one), this camera would show worse results in altimetry than planimetry.

3.3.4 Comparison of the averages of within-subject measures

Since we want to establish whether there are differences between the cameras, the right thing is to compare the results based on an operator individually. Keep in mind that the variability between operators may be greater than the variability between the cameras, each operator must be studied independently. In fact, just applying a simple hypothesis test corresponding to the homogeneity of variances, it is possible to observe that there are no significant differences between cameras while there are differences between operators. So, it would be wrong to use the *t* comparison test for the assessment of the precision of the two cameras, since there are not different operators, but the same operator measures with two different cameras. Therefore, we apply the t test comparison of the averages of within-subject measures, which should follow a normal distribution with mean zero. The null hypothesis, H_0, establishes that the different cameras do not affect the precision obtained. The alternative hypothesis, H_a, establishes that the different cameras modify the precision, and thus the mean difference is not zero.

$$\begin{aligned} H_0 &: \mu d = 0 \\ H_a &: \mu d \neq 0 \end{aligned} \tag{17}$$

The statistical test is constructed around the null hypothesis. It consists in comparing the difference average with the theoretical average, which is zero and represents no change. If calculating the difference average, the value obtained in the sample is not zero, the null hypothesis is rejected. That is, if there are differences between the observed and the null hypothesis, it is accepted that there are differences between cameras. Considering that the sample is large (n> 30) it is assumed that the dataset follows a normal distribution.

3.3.5 Analysis of agreement

The Pearson correlation coefficient, *r*, is usually applied to assess the concordance between the results obtained with different instruments. But this strategy would be incorrect in the present case since this coefficient renders the intensity of the linear association between two measures, and not the degree of agreement between them (Bland & Altman, 1986). A more correct strategy to measure the concordance is to calculate the Intraclass Correlation

Coefficient, *ICC* (Fleiss, 1986). Among the various *ICC* estimators, two of them are used in this paper: ICC_C to measure consistency, and ICC_A to measure absolute agreement (Doménech, 2005). Both ICC_C and r share the fact that are unable to discriminate a constant difference between two sets of observations, but ICC_C is sensitive to proportional differences and r, no. The ICC_A senses any difference between sets as an inconsistency, independently if this difference is constant, proportional or any other. The lower the value of ICC_A, the larger the disagreement is.

Considering i subjects and j values for these subjects, in order to calculate the *ICC*, the total variation (*SST*) of the i $*j$ observations must be decomposed in three terms: the variation due to subjects (*SSS*), the variation due to evaluators (*SSE*) and the residual variation (*SSR*):

$$SST = SSS + SSE + SSR \tag{18}$$

With the following degrees of freedom (*df*):

$$\begin{aligned} df_T &= i*j-1 \\ df_S &= i-1 \\ df_E &= j-1 \\ df_R &= (i-1)*(j-1) \end{aligned} \tag{19}$$

Afterwards, the mean values (*MS*) are computed dividing the sum of squares (SS) by their corresponding degrees of freedom. The ICC_A and the ICC_C are calculated according to the following expressions:

$$\begin{aligned} ICC_A &= \frac{i*(MSS-MSR)}{i*MSS + j*MSE + (i*j-i-j)*MSR} \\ ICC_C &= \frac{MSS-MSR}{MSS+(j-1)*MSR} \end{aligned} \tag{20}$$

In Figure 4 four different cases are outlined, showing a perfect linear relationship ($r=1$). In the top left, a case total agreement is showed, which is obtained when the valuations A and B are identical, and therefore the two evaluators values are 1. In the upper right, a case of constant disagreement is depicted, in which the consistency is 1 whereas the total agreement decreases. At the bottom, are showed the cases of proportional disagreement (left) and proportional and constant disagreement (right), where the difference between evaluators can be observed.

While consistency is behaving as an index of additivity the correlation coefficient is shown as an index of linearity. ICC_C and r both have in common a lack of sensitivity to contain a constant difference between two sets of observations, but differ in that ICC_C is sensitive to differences of proportional representation. The ICC_A provides any difference between measures with disagreement, whether they are of constant rate, proportional or otherwise. The lower the value of ICC_A, the more disagreement exists.

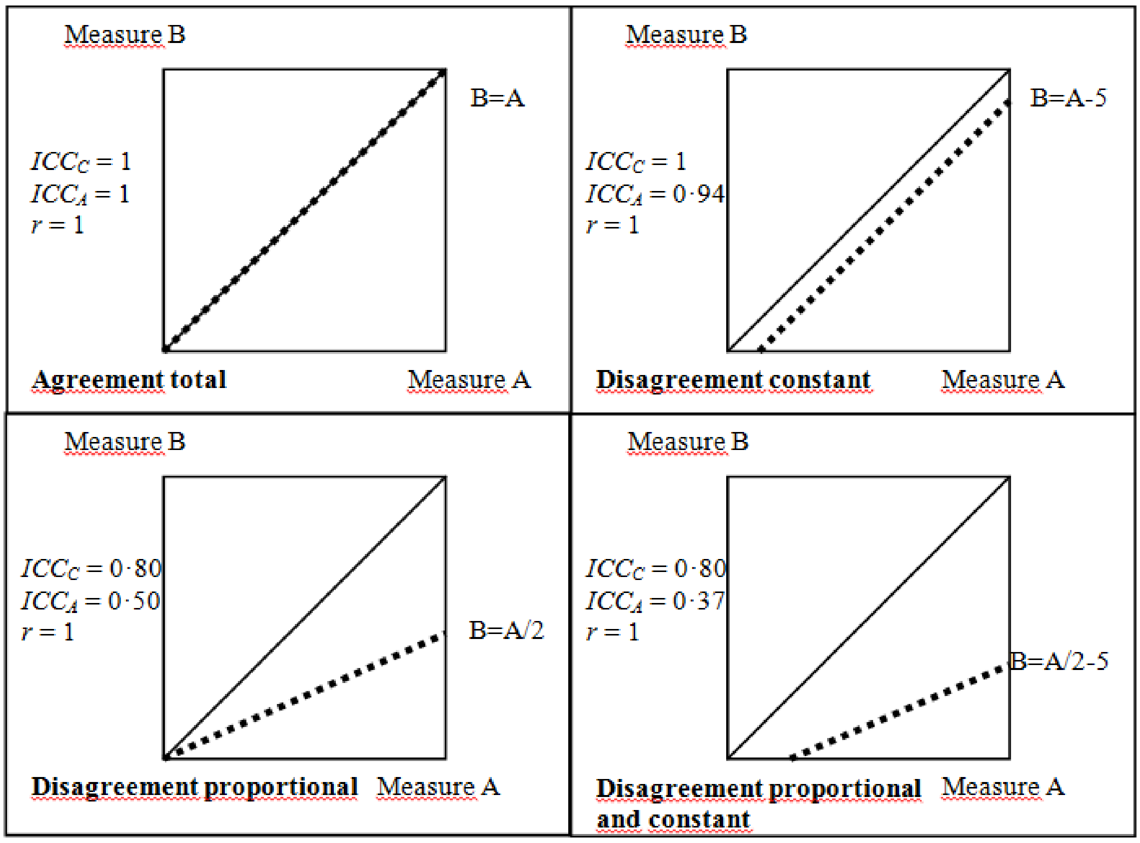

Fig. 4. Consistency, total agreement and linear correlation coefficient (Doménech, 2005).

3.3.6 Personal equation

As is known, errors can be classified as instrumental, natural or personal (Wolf & Ghilani, 1997):

- Instrumental errors: caused by imperfections in the construction or adjustment of the instruments.
- Natural errors: caused by the variation of environmental conditions.
- Personal errors: due to human limitations. The size of this error depends on personal ability and skill of each operator.

Aerial photogrammetry has always coped with the latter type of error in terms of personal equation, assuming this error as a systematic trend of each operator.

Stereoscopic measurements in the personal equation are used to compare film and digital cameras. It is expected that an operator who carries out the measures under the real situation of the point with film camera, do the same with digital camera. Even the relationship between personal equations of film and digital camera should reflect the theoretical ratio (*b/h*) between the two cameras.

A value for the "real" situation of a point can be calculated as the average of all the observations made by all operators at that point. The personal equation of each operator, Eq_i, can be obtained by the difference of his personal measure with the global measure of all operators (real situation):

$$Eq_i = A - a_i \tag{21}$$

where i is the operator, A is the average of all measurements of all operators to a certain point, and a_i is the average of all measurements at that point made by the operator i.

Logically, only those measures which imply the same operators observing the same points with film and digital camera will be presented and analyzed.

3.4 Relative relieves

The relief range of an area, ΔH, can be defined as the difference between the maximum and minimum height:

$$\Delta H = Zmax - Zmin \tag{22}$$

While the relative relieve is the ratio between the relief of an area and flight height, H, from which the images were taken:

$$Relative\ relieve = \frac{\Delta H}{H} \tag{23}$$

This relative relief indicates a degree of three-dimensional enhancement. The higher the relative relieve is the better is perceived the relief, but it also implies a greater variability in the positioning, and if the operator does not make good measurements, this would explain a larger standard deviation in a series of repeated measures. However, too large relative relieve should get worse the altimetric positioning due to effects of perspective, i.e., there must be an optimum value for which a greater precision is achieved in the altimetric positioning. Anyway, for the flights used in this work, it can be remarked that the higher the relative relieve, the better the stereoscopic positioning.

Considering two different flight heights for the two cameras, $H_A \neq H_D$, for the same study area, $\Delta H_A = \Delta H_D$, the relationship between the relieves on the two flights is simplified to the relationship between the two flight altitudes:

$$\frac{\left(\Delta H / H_A\right)}{\left(\Delta H / H_D\right)} = \frac{H_D}{H_A} \tag{24}$$

Then the ratio of heights of flight gives the variation of relative relieve between the two cameras. The following values can be obtained:

- $H_D/H_A > 1$: the relieve is noticed worse with the digital camera than with the film camera. This is the situation that occurs in most cases, since for the same *GSD*, $H_D > H_A$.
- $H_D/H_A < 1$: the relieve is noticed better with the digital camera than with the film camera.
- $H_D/H_A = 1$: the relieve is noticed equal for both cameras.

4. Experimental results

This section shows and analyzes the experimental results obtained with three different flights establishing a comparison between the stereoscopic precision obtained with film and digital cameras. Aspects such as: type of measurement, operator expertise, point type and area of the stereoscopic model, have been considered.

4.1 Flights

The flights used to undertake the stereoscopic measurements performed by operators are:

- “Laguna de Duero” (LD): this large scale flight play an essential role since establishes comparison between film camera (LD_AE) and digital camera (LD_D). In addition, this flight was observed with the original negatives (LD_AA) in an analytical photogrammetric station, Leica SD2000.
- “Mansilla de las Mulas” (MM): this large-scale flight was recorded only with digital camera (MM_D).
- “Arauzo” (AR): this small-scale flight performs as a comparison between film camera (AR_AE) and digital camera (AR_D).

Table 2 collects all these data.

Flight	Camera	m_b	px (µm)	GSD (m)	B (m)	H (m)	B/H	c (mm)
LD_AE	Leica RC30	5.000	20	0,100	450	767	0,587	153,42
LD_D	UltraCamD	8.333	9	0,075	225	845	0,266	101,40
MM_D	UltraCamD	11.111	9	0,100	300	1,125	0,267	101,40
AR_AE	Leica RC30	30.000	15	0,450	2,686	4,600	0,583	153,42
AR_D	UltraCamD	55.555	9	0,500	1,500	5,633	0,267	101,40

Table 2. Flight used for manual stereoscopic measurements, where m_b indicates the scale denominator of the photographs; *px*, the pixel size; *GSD*, the pixel projection over the ground; *B*, the base (ground); *H*, the flight height; *B/H*, the base-height ratio; and *c*, the focal length of the camera.

4.2 Hypothesis

4.2.1 Measurements

For every point and operator, the standard deviation in *XY*, S_{XY}, has been obtained and also the standard deviation in *Z*, S_Z. These are parameters to be analyzed and considered to express the precision of the stereoscopic (both planimeric and altimetric) measures, as expressed by Hallert (1959) on repeated direct measurements of unknown quantities.

It is not aimed to asses the global precision of a photogrammetric product but the precision related to the stereoscopic model (Kraus, 1993). The point stereoscopic measurements have been done in this order: first point, second point and so on until the last point to complete one cycle. No point has been observed *n* times in a consecutive fashion. To achieve *n* measurements of the same point, the cycle has been repeated *n* times. Each operator has realized 3 cycles at the beginning of the day and 3 cycles again at midday, to avoid tiredness in his performance, the repeatability in measurements and the so called learning effect. In this way, 6 measurements per point and operator have been obtained for a total of 13 operators from public and private companies. These stereoplotter operators are daily engaged in purely stereoscopic photogrammetric procedures (stereoplotting, editing DTMs) and have an experience that ranges from 10 years (high) to 5 years (medium) and to 1-2 years (low). In any case the minimum experience to achieve significant results has been considered to be one year.

Due to the modular composition of large format digital cameras (DMC and UltraCamD) it has been considered relevant to perform a geometric analysis based on the distribution of the points across the stereoscopic area. Consequently, the points have been distributed in nine zones of the stereoscopic model. On each of these nine zones, at least one of the three following types of points has been measured: well defined points on the terrain; easy urban points (roofs) and difficult urban points (ground points close to buildings).

4.2.2 Types of points

For the different cases of study three types of points have been considered:

- Well-defined terrain points.
- Well-defined urban points (roofs and curbs, both above and below).
- Difficult urban points (ground points close to buildings).

4.2.3 Area of the stereoscopic model

Given the modular structure of the images coming from large-format digital cameras, a geometric analysis has been performed based on the location of points within the stereoscopic model. Therefore, the points shall be distributed in nine areas of the stereoscopic model, to analyze the influence of the position of point in the model. In each one of these areas at least one point of each type will be chosen (Fig. 5).

1	2	3
4	5	6
7	8	9

Fig. 5. Numbering of areas within the stereoscopic model.

4.3 Case study 1: Large-scale flight Laguna de Duero (LD)

In the stereoscopic model obtained with the film camera, Leica RC30 (LD_AE), in Laguna de Duero, 46 points have been observed. These measurements were made by five different operators in two sets of three cycles each. The five operators were distributed as follows: 2 with high experience, 1 with medium experience and 2 with low experience:

Operator	S_{XY} *(m)*	S_Z *(m)*	*Number of observations*
1	0,013	0,025	274
2	0,018	0,042	276
3	0,012	0,030	268
4	0,020	0,033	276
5	0,018	0,030	275
Average	0,016	0,032	Total 1.369

Table 3. Precision obtained with the flight LD_AE.

These same operators observed the same points in digital images for the Laguna de Duero flight using the UltraCamD digital camera (LD_D):

Operator	S_{XY} *(m)*	S_Z *(m)*	*Number of observations*
1	0,014	0,042	274
2	0,018	0,070	274
3	0,011	0,048	275
4	0,019	0,063	276
5	0,017	0,053	273
Average	0,016	0,055	Total 1.372

Table 4. Precision obtained with the flight LD_D.

4.3.1 Film-digital flight comparison: LD_D vs. LD_AE

The ratio of S_{XY} for the two flights is unity (0,016/0,016), so there are significant differences in planimetry. The ratio of Z precision is determined empirically as 1,719 (0,055/0,032). While the ratio given theoretically is:

$$\frac{(\sigma_z)_{LD\_D}}{(\sigma_z)_{LD\_AE}} = \frac{\left(\frac{0{,}075m}{k} * \frac{101{,}4mm}{27mm}\right)_{LD\_D}}{\left(\frac{0{,}100m}{k} * \frac{153{,}42mm}{88mm}\right)_{LD\_AE}} = 1{,}616 * \frac{k_{LD\_AE}}{k_{LD\_D}} \tag{25}$$

Comparing the observed with the theoretical, it results $k_{LD\_AE} = 1{,}06 * k_{LD\_D}$ (6%). It concludes that there are only slight variations in the precision with digital camera than with the film camera.

Are these empirical dataset concluding? Yes, very concluding, since they encompass 5 operators, with different experience and measuring the same points with film and digital camera. In addition, these points are well distributed throughout the model and represent all types of points.

What might be due this slight difference? The relative relieve is the ratio between the relieve of an area and the flight altitude from which the images were taken ($\Delta H/H$). The relative ratio between relieves indicates the variation between the relative relieve between both cameras:

$$\frac{\left(\Delta H/H\right)_D}{\left(\Delta H/H\right)_{AE}} = 0{,}90 \tag{26}$$

This indicates that the digital flight observes the relieve a 10% flatter than the film flight. This value may explain the difference of 6% previously observed.

4.3.2 Average differences for the S_{XY}: LD_D vs. LD_AE

Using the comparison of the averages of within-subject measures introduced in the previous section, Table 5 outlines the comparison of averages for the standard deviation in XY.

Operator	*Average differences (mm)*	*Confidence interval (lower; upper) (mm)*	*p-value*
1	0,587	-3;4	0,771
2	-0,348	-5;4	0,880
3	-0,565	-3;2	0,694
4	-0,652	-6;5	0,813
5	-0,522	-6;5	0,850

Table 5. Comparison of averages for S_{XY}: LD_D vs. LD_AE. Confidence level of 95%.

In view of the differences in S_{XY} between the flights LD_D and *LD_AE* (operators 1 to 5), one can make the following observations:

- The differences averages are less than a millimeter for all operators and, except for the first one, they are negative, which means that the S_{XY} of LD_D is larger than the S_{XY} of LD_AE.
- The 95% confidence intervals of the differences averages provide interesting ranges. All of them are, approximately, symmetric intervals centred on zero. This is consistent with the fact that there are no really differences between the cameras.
- There are no significant differences for any operator, for a significance level of 5%.

4.3.3 Average differences for S_Z: LD_D vs. LD_AE

The following table (Table 6) shows the data for comparison of averages for the standard deviation in *Z*.

Operator	*Average differences (mm)*	*Confidence interval (lower; upper) (mm)*	*p-value*
1	17,761	11; 24	0,000
2	28,739	10; 47	0,003
3	18,304	7; 28	0,001
4	29,652	19; 39	0,000
5	23,587	13; 33	0,000

Table 6. Comparison of averages for S_Z: LD_D vs. LD_AE. Confidence level of 95%.

In view of the differences in S_Z between the flights LD_D and LD_AE (operators 1 to 5), one can make the following observations:

- The differences averages range from 17,761mm for the operator 1 to 29,652 mm for the operator 4. For all operators, the differences averages are positive, which means that the S_Z of LD_D is larger than the S_Z of LD_AE.
- None of the 95% confidence intervals of differences means contains zero.
- There are significant differences in all operators, for a significance level of 5%.

4.3.4 Analysis of agreement: LD_D vs. LD_AE

As in the previous case this comparison element can be applied only on the flights that were observed by the same operators. The results are collected in Table 7.

	S_{XY}	S_Z
ICC_C	0,835 (p=0,019)	0,854 (p=0,015)
ICC_A	0,735 (p=0,019)	0,288 (p=0,015)
r	0,893 (p=0,021)	0,988 (p=0,001)

Table 7. LD_D vs. LD_AE: ICC_C: consistency; ICC_A: total agreement; r: linear correlation coefficient, p: p-value: contrast significance of the differences average. Confidence level of 95%.

In case of the data from flights LD_D vs. LD_AE, the relationship between the values of S_{XY} shows a good agreement, consistent and linear, although there is a slight constant discrepancy. The relationship between the values S_Z shows a low agreement but consistent and linear. This indicates that in the relationship between the values of S_Z there is a proportionate and constant inconsistency

4.3.5 Personal equation: LD_D vs. LD_AE

The personal equation of each operator Z has been calculated for each point, as explained above (expression 21), from the observations performed in LD_D and LD_AE. The average data are shown in Table 8:

Operator	*LD_D (mm)*	*LD_AE (mm)*	*LD_D/LD_AE*
1	-32	-16	2,0
2	84	55	1,5
3	-109	-43	2,5
4	86	21	4,1
5	-29	-18	1,6

Table 8. Average values of the personal equation for the operators who performed the measurements for LD_AE and LD_D.

Those values in the right column (Table 8) which differ from the unit mean that an operator behaves differently with the two cameras.

These average values per operator in the personal equation shows that the behavior of an operator in film measures is transmitted to digital measures, reflecting the same sign and a ratio (LD_D/LD_AE) between 4,1 and 1,5.

In order to analyze in detail the personal equation and its variation between cameras, the test of average differences has been applied. The following table (Table 9) summarizes the results of this comparison of paired samples.

Operator	*Average differences (mm)*	*Confidence interval (lower; upper) (mm)*	*p-value*
1	-16	-32;1	0,059
2	29	-3;60	0,075
3	-66	-83;-49	0,000
4	64	46;82	0,000
5	-12	-25;2	0,086

Table 9. Test results: comparison of averages differences for the personal equation of the operators who performed observations on flights LD_AE and LD_D. Confidence interval 95%.

In view of the hypothesis testing for differences in personal equation, the following observations can be pointed out:

- The averages differences range from -66 mm for the Operator 3 to 64 mm for the Operator 4. In three cases (operators 1, 3 and 5), the average difference is negative, but this does not mean that the personal equation is greater for LD_D than for LD_AE, but this value is because the personal equation for these operators is negative in both cases (note the data of personal equation for operator in Table 9).
- The confidence intervals at 95% for the averages differences for the operators 1, 2 and 5 contain the zero value, but they are markedly asymmetric, while the intervals of the operators 3 and 4 do not include zero.
- In line with the comments in the previous section, there are no significant differences for a significance level of 5% for the operators 1, 2 and 5, but they show very low values, which suggests that there are differences. For the other two operators it can be said clearly that there are differences between cameras.

4.3.6 Other considerations: LD_D vs. LD_AE

Two more additional considerations should be remarked. The first consideration is based on the location of the points where the measures are performed. In order to get the same ground sample distance (*GSD*) with film and digital camera, it is necessary to use several digital camera models that cover the same area recorded by a film camera. The second consideration is related with the type of point. Especially in the case of difficult points distributed on the bottom of the buildings, the precision will get worse in Z for digital camera.

Type of point	S_{XY}_LD_AE (m)	S_{XY}_LD_D (m)	S_Z_LD_AE (m)	S_Z_LD_D (m)
T	0,014	0,017	0,029	0,052
U_S	0,015	0,014	0,033	0,050
U_C	0,024	0,017	0,042	0,074

Table 10. Precision obtained with flights LD_D and LD_AE, with different types of points: *T*: well-defined terrain points; *U_S*: Well-defined urban points; *U_C*: Difficult urban points.

These two considerations suggest that the measures will not be performed equally for both cameras.

What would it happen if the scanning resolution for film images were 15 µm instead of 20 µm? In this case the pixel size on the ground for the film camera would be 0,075 m. A value similar to the digital flight, so that the theoretical ratio of altimetric precision would be as follows:

$$\frac{(\sigma_z)_{LD\_D}}{(\sigma_z)_{LD\_AA}} = \frac{\left(\frac{0{,}075m}{k} * \frac{101{,}4mm}{27mm}\right)_{LD\_D}}{\left(\frac{0{,}075m}{k} * \frac{153{,}42mm}{88mm}\right)_{LD\_AA}} = 2{,}155 * \frac{k_{LD\_AA}}{k_{LD\_D}} \tag{27}$$

This value of 2,155 is very different (about 33%) from its theoretical, 1,616. Nevertheless, if these same 5 operators perform their measures with a 15 µm image, do the empirical precision would be 33% better? Several authors believe that the optimal size is 15 µm scan (Boniface, 1996). The next section addresses this question.

Note that for changing the *GSD* size (15 to 20 µm) with film camera is not necessary to change any parameters of the proposed flight, but simply the scanning pixel size. Neither the focal length or the frame size or resolution of the film, etc.

4.3.7 Comparison of: LD_AE vs. LD_AA

In this case, manual measures were performed over the same points considering the original images, using a Leica SD2000 analytical plotter with analog vision system, but with other operators in the restitution. This is the flight LD_AA.

Operator	S_{XY} (m)	S_Z (m)	*Number of observations*
1	0,012	0,021	275
2	0,019	0,031	269
3	0,012	0,020	276
4	0,011	0,027	274
Summary	0,014	0,025	1094

Table 11. Precision obtained with the flight LD_AA.

The *XY* precision ratio shows a decrease of 14% (0,016/0,014) with the image scanned at 20 µm.

This may indicate that a pixel scan size of 17,5 µm (20/1,14) would have been optimal. The results come to confirm that with a scanned resolution of 20 µm the *Z* precision is about 28% (0,032/0,025) worse than with the original images. According to this data and considering that the scan size is the main factor, the optimal size would have been of 15,6 µm (20/1,28). (In this case, the theoretical reason σ_Z is 1 since it is the same camera).

These data seem to indicate that more precision could have been obtained if the images had been scanned at 15 µm. With this, the *GSD* (0,10 m) would have been the same for the film and digital camera.

Note that the measure instrument is completely different (including the stereoscopic system). In addition, measures were made with different operators. Probably, those differences encountered during the experiments could be related with these variables.

4.3.8 Comparison: LD_D vs. LD_AA

If we work with global average values for both flights, a comparison can be established, even knowing the differences between measurements (different instrument and different operators). The *XY* precision ratio is observed to be about 14% (0,016/0,014) more accurate for film flight. The theoretical precision in Z, considering the same *GSD* for both flights, is of 2,155, while the empirical precision is 2,200 (0,055/0,025), almost the same.

4.4 Case study 2: Large-scale flight Mansilla de las Mulas (MM)

Due to initial requirements for the selection of points and the type of points, it is not clear the precision related with those flights executed with low height. For this purpose, several measures were performed for a digital flight, MM_D, using a different collection of points and with a 0,10 m *GSD*. In this case, only well-defined terrain points were observed, distributing three points along the nine areas of the stereoscopic model. The operators were four: 2 with high experience, 1with medium experience and 1 with low experience (Table 12).

Comparing LD_AE vs. MM_D, the difference for *XY* precision reaches the 13% (0,018/0,016), when the *GSD* is the same. The ratio for *Z* precision is determined empirically as 1,594 (0,051/0,032), while the ratio determined theoretically, having the same *GSD*, is 2,155. As a result, the digital flight MM_D is a 35% better than the film flight LD_AE (k_{MM_D} = 1.35 * k_{LD_AE}) considering a pixel size of 20 microns.

Operator	*Sxy (m)*	*Sz (m)*	*Number of observations*
1	0,016	0,053	162
2	0,018	0,046	162
3	0,022	0,062	162
4	0,016	0,044	162
Average	0,018	0,051	Total 808

Table 12. Precision obtained with the flight MM_D.

Comparing LD_AA vs. MM_D, the difference in XY precision is 28% (0,018/0,014), while the Z empirical precision is 2,040 (0,051/0,025), pretty much the same than the Z theoretical precision, 2,155.

4.5 Comparison between large-scale flights

The following table (Table 13) shows a series of data representative of each flight which allow us to make comparisons between flights.

	LD_AE RC30-D	*LD_AA RC30-A*	*LD_D ULC-D*	*MM_D ULC-D*
S_i (μm)	3,20	2,80	1,92	1,62
px (μm)	20	15	9	9
K	6,25	5,37	4,69	5,56
S_{XY}/GSD	0,16	0,19	0,21	0,18
S_Z/H ($x10^{-5}$)	4,17	3,26	6,53	6,03
$(S_{XY}/S_Z)/(B/H)$	0,85	0,95	1,09	1,32

Table 13. Data coming from the large-scale flights analyzed.

In the table 13: Si: image measures precision in micrometers, px: pixel size in microns; k: precision indicator; S_{XY}/GSD: ratio between planimetric precision and GSD, S_Z/H: ratio between altimetric precision and flight height; $(S_{XY}/S_Z)/(B/H)$ quotient between the planimetric and height empirical standard deviations ratio and the planimetric and height theoretical precision ratios. Note that it has been assumed that the px of LD_AA, the film flight observed with the analytical stereoplotter, is 15 μm.

The values of S_i and px are not comparable, whereas the indicators of precision, k are comparable. It must be emphasized the equality between MM_D and LD_AA. The minor value for the digital camera flight LD_D could be related with the selection and type of points, while best values reached for film camera flight LD_AE, may be due to the pixel size of 20 μm. The ratios S_{XY}/GSD are similar for all flights. The ratios S_Z/H for film camera flights are around $3\text{-}4{*}10^{-5}$ (0,00003), while for the two digital flights are around $6{*}10^{-5}$.

For both film flights the quotient $(S_{XY}/S_Z)/(B/H)$ indicates that the planimetric precision is better than the altimetric precision, whereas for the digital flights the quotient expresses the opposite.

4.6 Case study 3: Small-scale flight Arauzo

A case of study was performed in Arauzo (Spain), using a small-scale and combining film camera (AR_AE) and digital camera (AR_D). In particular, for the film flight, AR_AE, 3 points were measured along the 9 areas of the stereoscopic model (a total of 27 points). The points were observed by four different operators in 2 sets of 3 cycles each. The measured points were well-defined terrain points, since the workspace was rural. The experience of the operators was distributed as follows: 2 with high experience, 1 with medium experience and 1 with low experience. Table 14 outlines the main results.

Operator	S_{XY} *(m)*	S_Z *(m)*	*Number of observations*
1	0,093	0,132	162
2	0,093	0,125	162
3	0,104	0,214	161
4	0,084	0,119	162
Summary	0,094	0,148	647

Table 14. Precision obtained with the film flight AR_AE.

The digital flight AR_D was observed by these same four operators, which measured the same points.

Operator	S_{XY} *(m)*	S_Z *(m)*	*Number of summary*
1	0,124	0,228	162
2	0,086	0,221	161
3	0,145	0,311	162
4	0,110	0,229	162
Summary	0,116	0,247	647

Table 15. Precision obtained with the digital flight AR_D.

4.6.1 Comparison between film and digital flight: AR_AE vs. AR_D

Comparing the precision obtained, it can see that the planimetric ratio S_{XY} (0,116/0,094) is 23% worse with the digital camera, even when the difference between *GSD* is only 11% (0,500/0,450). It is important to point out the uncertainty in the point definition given the rustic area. The ratio of Z precision is determined empirically as 1,669 (0,247/0,148), while the ratio if Z precision determined theoretically is 2,393. This implies that k_{AR_D} = 1,43 * k_{AR_AE}:

$$\frac{(\sigma_z)_{AR\_D}}{(\sigma_z)_{AR\_AE}} = \frac{\left(\frac{0{,}500m}{k} * \frac{101{,}4mm}{27mm}\right)_{AR\_D}}{\left(\frac{0{,}450m}{k} * \frac{153{,}42mm}{88mm}\right)_{AR\_AE}} = 2{,}393 * \frac{k_{AR\_AE}}{k_{AR\_D}} \tag{28}$$

It concludes that the precision in Z with the digital camera is better (43%) than the precision in Z determined with the film camera. The variation of relative relieve between flights is 22%. The lower relative relieve, the lower range of variability in Z positioning, so that the standard deviation will be less. Also, the difference in relative relieve must be considered in relation to the different focal distances. The longer the focal length the flatter is the relieve.

Note that one important factor which could be minimizing the effect of the ratio *B/H* is the increase of flight height.

The following table (Table 16) collects representative data for each flight:

	AR_A	*AR_D*
S_i (μm)	3,13	2,09
Px (μm)	15	9
K	4,79	4,31
S_{xy}/GSD	0,21	0,23
$S_z/H(x10^{-5})$	3,22	4,38
$(S_{xy}/S_z)/(B/H)$	1,09	1,76

Table 16. Data from the four flights analyzed large-scale.

The ratio S_{XY}/GSD is not very different for both flights (0,21 and 0,23), as well as the altimetric ratio S_Z/H (3,22*10^{-5} and 4,38*10^{-5}). The quotient $(S_{XY}/S_Z)/(B/H)$ show for both flights that the planimetric precision is lower than the altimetric precision, even though in the case of digital camera is much more pronounced this difference.

4.6.2 Average differences for S_{XY}: AR_D vs. AR_AE

The following table (Table 17) shows the average differences for S_{XY}:

Operator	*Average diferences (mm)*	*Confidence interval (lower; upper) (mm)*	*p-value*
1	30,444	-23; 84	0,255
2	-7,000	-32; 18	0,574
3	40,778	-4; 85	0,074
4	26,222	-27; 79	0,322

Table 17. Comparison of averages for S_{XY}: AR_D vs. AR_AE. Confidence level of 95%.

The following observations can be made for S_{XY} according to the hypothesis testing:

- For the operators 1, 3 and 4 the average difference is positive, this implies that for these operators *Sxy_AR_D*> *Sxy_AR_AE*. This is not the case for the operator 2 since its performance is opposite.
- The confidence interval 95% for the average differences containing zero, but show a clear asymmetry.
- For a significance level of 5%, no significant differences were found for any operator.

4.6.3 Average differences for S_Z: AR_D vs. AR_AE

The following table (Table 18) shows the average differences for S_Z.

Operator	*Average differences (mm)*	*Confidence interval (lower; upper) (mm)*	*p-value*
1	95,630	61;129	0,000
2	95,481	48; 142	0,000
3	97,037	33;161	0,004
4	110,111	75;145	0,000

Table 18. Comparison of averages for S_Z: AR_D vs. AR_AE. Confidence level of 95%.

According to the hypothesis testing, the following observations can be made for *Sz*:

- For all operators, the average difference is positive, this implies that *Sz_R_D>Sz_ AR_AE*. In addition, the average differences are between 95,481 mm and 110,111 mm.
- None of the confidence intervals of 95% for the average difference contains zero. All ranges implies that *Sz_AR_D>Sz_AR_AE*.
- There are significant differences in all operators, for a significance level of 5%.

4.6.4 Analysis of agreement: AR_D vs. AR_AE

The total agreement, the consistency and the correlation coefficient are depicted in the Table 19.

	S_{XY}	S_Z
ICC_C	0,620 (p=0,132)	0,940 (p=0,009)
ICC_A	0,347 (p=0,132)	0,295 (p=0,009)
r	0,658 (p=0,171)	0,986 (p=0,007)

Table 19. AR_D vs. AR_AE: ICC_C: consistency; ICC_A: total agreement; r: linear correlation coefficient. Confidence level of 95%.

Note that S_{XY} values are not significant for a confidence level of 95%. On the other hand, the relationship between S_Z shows a low total agreement but following a consistent and linear trend.

4.6.5 Personal equation: AR_D vs. AR_AE

The following table (Table 20) shows the personal equation results for each operator and based on the observations performed for flights: AR_AE and AR_D.

The values provided by personal equation do not show a clear trend. Even their heterogeneity might indicate that the data are unreliable. In particular, for the operator 1 and 3 the sign is changed, indicating that the altimetric positioning is made above the terrain for digital flights and bellow the terrain for film flights. However, it is important to remark that the average altimetric position of a point is obtained from the average measures of all operators, so that the change of sign should be interpreted as an increase in the personal equation difference between film and digital camera.

Operator	*AR_D (mm)*	*AR_AE (mm)*	*AR_D/AR_AE*
1	90	-20	-4,5
2	-32	-64	0,5
3	-279	12	-23,5
4	222	72	3,1

Table 20. Personal equation for the operators who performed the measurements in flights: AR_D and AR_AE.

The following table (Table 21) summarizes the results of this comparison of differences for personal equations for each operator and for each point.

Operator	*Average (mm)*	*Confidence interval (lower; upper) (mm)*	p-value
1	110	49;110	0,001
2	31	-22;85	0,236
3	-291	-386;-196	0,000
4	150	62;237	0,002

Table 21. Test results comparing average differences for the personal equation of the operators who made observations on flights AR_D and AR_AE. Confidence level of 95%.

For a significance level of 5%, differences between cameras are found for the operators 1, 3 and 4, whereas no differences are found for the operator 2.

5. Conclusions

In this chapter, an assessment of stereoscopic precision for large-format digital cameras has been studied. In all the flights, the influence of a set of variables on the precision in *XY* and in *Z* has been analyzed. These variables are: the distribution of points in the model; the operators and their experience; and the type of points.

In particular, in every case the planimetric ratio S_{XY}/GSD indicate that the planimetric error is similar for both flights. Besides this, it is supposed that the flight height is independent, even for large flight heights. The altimetric error seems to indicate that the main difference comes form the flight height and in minor level from the relation *b/h*. No significant differences are observed in the ratio S_Z/H for all flights analyzed.

In conclusion, the approach of relating digital and film flights through the *GSD* is right on the planimetric side. However, the altimetric precision must be analyzed carefully in order to determine if it is possible to maintain traditional flight heights. In this sense, the indicators of precision *k*, as a fraction of the pixel of the image, are a good comparator.

The values for the quotient $(S_{XY}/S_Z)/(B/H)$ show that those film flights provide slightly better results for planimetry than for altimetry, while in the case of digital camera just the opposite occurs, having worse planimetric precision.

The empirical conclusion that seems to be reached is that the negative impact on altimetric precision caused by the lower ratio *B/H* for digital camera flights is lower when the flight height increases.

In summary, the main conclusion to be drawn on the stereo manual measurements is that the planimetric accuracy is the same for both cameras: film and digital. However, altimetric precision does not provide the same results, being the ratio *b/h* the main cause of the difference between both cameras.

6. References

Alamús, R., Kornus, W., Palà, V., Pérez, F., Arbiol, R., Bonet, R., Costa, J., Hernández, J., Marimon, J., Ortiz, M.A., Palma, E., Pla, M., Racero, S., Talaya, J. (2005). Validation process of the ICC digital camera. *Proceedings of ISPRS Workshop on High-Resolution Earth Imaging for Geospatial Information*, Hannover (Germany), May 2005.

Arias, B. & Gómez-Lahoz, J. (2009). Testing the stereoscopic precision of a large-format digital camera. *The Photogrammetric Record*, Vol. 24, Issue 126 (June 2009), pp 157–170, ISSN 1477-9730.

Blachut, T.J. (1955). General report of commission IV Subcommission IV/3. Small scale mapping. *Photogrammetria*, Vol. 12 (1955), pp 220-229, ISSN 0031-8663.

Bland, M. & Altman, D.G. (1986). Statistical methods for assessing agreement between two methods of clinical measurement. *Lancet*, Vol. i (1986), pp 307-310, ISSN 0140-6736.

Boniface, P. R. (1996). State-of-the-art in SoftCopy Photogrammetry, in: *Digital Photogrammetry: An Addendum to the Manual Photogrammetry*, C. Greve, American Society of Photogrametry and Remote Sensing, ISBN 978-1570830372, Bethesda, EEUU.

Commission C., O.E.E.P.E. (1955). Zeitlicher Ablauf der Messungen Deroulment chronologique des observations. *Photogrammetria*, Vol. 12 (1955), pp 198-199, ISSN 0031-8663.

Dörstel, C. (2003). DMC - Practical experiences and Photogrammetric System Performance, *Proceedings of Photogrammetric Week*, pp 59-65, Stuttgart (Germany), 2003.

Doménech, J.M. (2005) *Medida del cambio: Análisis de diseños con medidas intrasujeto. Medida de la Concordancia. Fundamentos de diseño y estadística, 14*. Signo, ISBN 9788480493017, España.

Dubuisson, B. (1955) Rapport général de la commission IV Sous-Commission. IV/2 Etablissement des plans des territoires urbains. *Photogrammetria*, , Vol. 2 (1955), pp 208-219, ISSN 0031-8663.

Fleiss, J.L. (1986). The design and analysis of clinical experiments. John Wiley & Sons, ISBN 978-0471820475, New York, EEUU.

Förstner. (1955). O.E.E.P.E., Commission C Rapport sur la restitution effectuée dans l'Institut für Angewandte Geodäsie, Francfort sur le Main Terrain d'essai d'Oberriet les vols Nr 1 et 3 (groupe I). *Photogrammetria*, , Vol. 12 (1955), pp 183-190, ISSN 0031-8663.

Gotthardt, E. (1955). O.E.E.P.E., Commission C Compte rendu de la restitution à la Technischen Hochschule, Stuttgart, des vols d'essai du gruope I du terrain d'Oberriet. *Photogrammetria*, , Vol. 12 (1955), pp 163-171, ISSN 0031-8663.

Gotthardt, E. (1958). Report on the First Results of Photogrammetric Test Performed near "Oberriet" by Commission C of the O.E.E.P.E. *Photogrammetria*, , Vol. 15 (1958), pp 141-148, ISSN 0031-8663 .

Grifoni, B. (1949) On different grade of precision attained in plotting using glass plate and film cameras. *Photogrammetria*, , Vol. 6 (1949), pp 55-58, ISSN 0031-8663.

Härry, H. (1954). La situation actuelle dans la mensuration cadastrale photogrammétrique. *Photogrammetria*, , Vol. 11 (1954), pp 45-50, ISSN 0031-8663.

Härry, H. (1955). Rapport général de la Commission IV Sous-Commission IV/1. Application de la photogrammétrie aux mensurations cadastrales et aux remaniements parcellaires. *Photogrammetria*, , Vol. 12 (1955), pp 203-207, ISSN 0031-8663.

Karara, H.M. (1967). Mono versus stereo analytical photogrammetry—theoretical considerations and experimental results. *Photogrammetria*, Vol. 22, Issue 3 (March 1967), pp 99-113, ISSN 0031-8663.

Krakau, C.E.T. (1970). A device for the automatic. Continuous recording of stereoscopic visual acuity. *Photogrammetria*, , Vol. 25, Issue 4 (February 1970), pp 115-123, ISSN 0031-8663.

Kraus, K., (1993). *Photogrammetry Vol. 1. Fundamentals and standard processes* (4th edition), Dümmler, ISBN 3427786846, Bonn, Germany.

Lehmann, G. (1955). Report on the work hitherto archieved by Commission C of the O.E.E.P.E. *Photogrammetria*, , Vol. 12 (1955), pp 156-163, ISSN 0031-8663 .

O'Connor, D. (1967). Some factors affecting the precision of coordinate measurements on photographic plates. *Photogrammetria*, Vol. 22, Issue 3 (March 1967), pp 77-97, ISSN 0031-8663.

Schiewe, J. (1995). Cartographical Potential of MOMS-02/D2 Image Data. In: Photogrammetric Week´95. Heidelberd: Ed. Fritsch/Hobbie, Wichmann. pp 99-105.

Spreckels, V., Syrek, L., Schlienkamp, A. (2010). DGPF Project: Evaluation of Digital Photogrammetric Camera Systems – Stereoplotting. *Photogrammetrie - Fernerkundung - Geoinformation*, Vol. 2010, No. 2 (May 2010), pp. 117-130, ISSN 1432-8364.

Stark, E. (1975). The effect on angular field on horizontal and vertical accuracy in photogrammetric plotting. *Procedings of Photogrammetric Week*, pp 129-145, Stuttgart (Germany), 1975.

Stickler, C.A. (1959). Interpretation of the results of the O.E.E.P.E. commission C. *Photogrammetria*, , Vol. 16 (1959), pp 8-12, ISSN 0031-8663.

Stoch, L. (1961). Note on C. A. Stickler's Paper. *Photogrammetria*, Vol. 18 (1961), pp 34, ISSN 0031-8663.

Trinder, J.C. (1986). Potentials of monocular and stereoscopic observations on aerial photographs. *Photogrammetria*, Vol. 41, Issue 1 (October 1986), pp 17-27, ISSN 0031-8663.

Wolf, P.R. & Ghilani, C.D. (1997). *Adjustment computations: statistics and least squares in surveying and GIS*. Ed. John Wiley and Sons,ISBN 0471168335, New York, EEUU.

Zorn, H. C. (1965). An instrument for testing stereoscopic acuity. *Photogrammetria*, Vol. 20, Issue 6 (December 1965), pp 229-238, ISSN 0031-8663 .

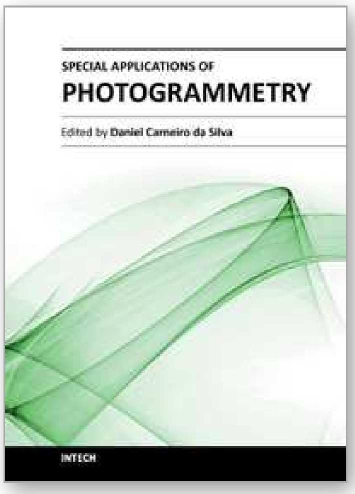

Special Applications of Photogrammetry

Edited by Dr. Daniel Carneiro Da Silva

ISBN 978-953-51-0548-0
Hard cover, 136 pages
Publisher InTech
Published online 25, April, 2012
Published in print edition April, 2012

Photogrammetry is widely accepted as one of the best surveying methods to acquire tridimensional data without direct contact with the object, but its high operational costs in equipment and personnel somewhat limit its application in mapping. However, with the development of digital photogrammetry in the 1990's, it was possible to introduce automated processes and reduce the personnel costs. In the following years, the cost of computer hardware, digital cameras and positioning sensors has been lowering, making photogrammetry more accessible to other engineering fields, such as architecture, archeology and health fields. This book shows the results of the work of researchers from different professional backgrounds, which evaluate the uses of photogrammetry, including issues of the data, processing, as well as the solutions developed for some surveying types that can be extended to many applications.

InTech Europe
University Campus STeP Ri
Slavka Krautzeka 83/A
51000 Rijeka, Croatia
Phone: +385 (51) 770 447
Fax: +385 (51) 686 166
www.intechopen.com

InTech China
Unit 405, Office Block, Hotel Equatorial Shanghai
No.65, Yan An Road (West), Shanghai, 200040, China
中国上海市延安西路65号上海国际贵都大饭店办公楼405单元
Phone: +86-21-62489820
Fax: +86-21-62489821